Electronic Supplementary Information (ESI)

Liquid Metal-Fluoropolymer Artificial Protective Film Endow Robust Lithium Metal Battery at Sub-zero Temperatures

Hongbao Li,‡ Rong Hua,‡ Yang Xu,‡ Da Ke, Chenyu Yang, Quanwei Ma, Longhai Zhang, Tengfei Zhou, Chaofeng Zhang**

Institutes of Physical Science and Information Technology, Leibniz Joint Research Center of Materials Sciences, Anhui Graphene Engineering Laboratory, Key Laboratory of Structure and Functional Regulation of Hybrid Material (Ministry of Education), Anhui University, Hefei 230601, China.

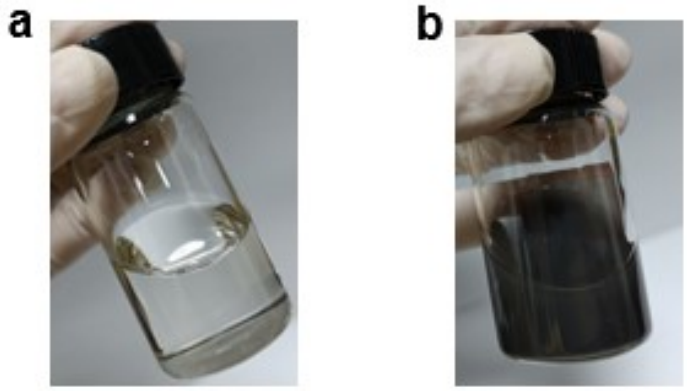

Figure S1. Suspension solutions of different components of (a) SPF and (b) LM-SPF (contain LM).

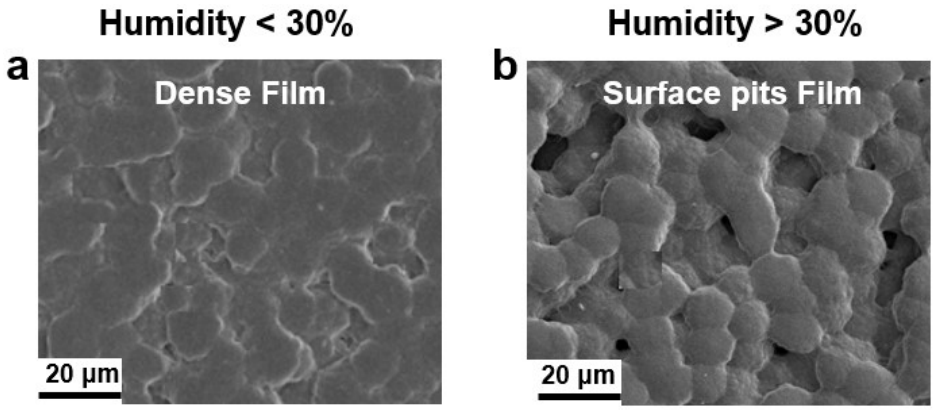

Figure S2. The SEM images of composite films with different morphologies.

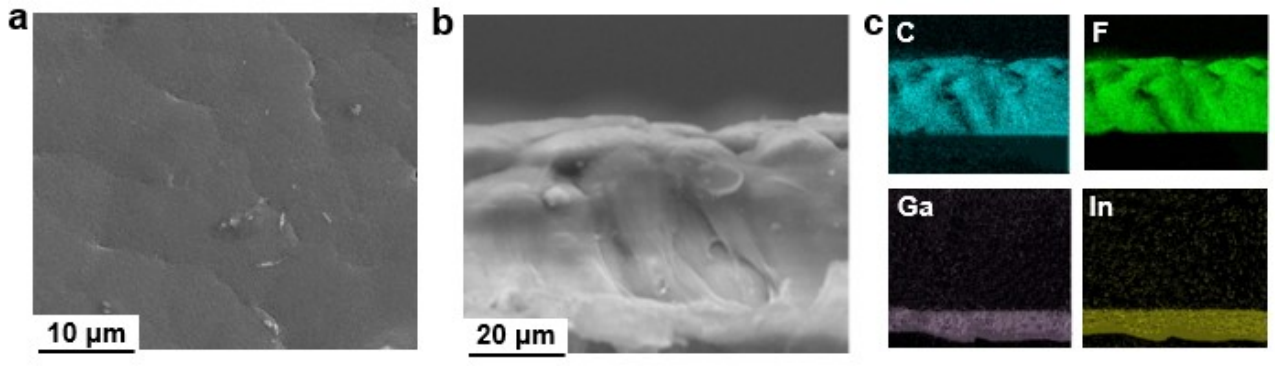

Figure S3. SEM images of (a) the lower side, (b) the cross section of the LM-SPF, and (c) elemental mapping of carbon (blue), fluorine (green), gallium (purple), and indium (yellow) of the LM-SPF.

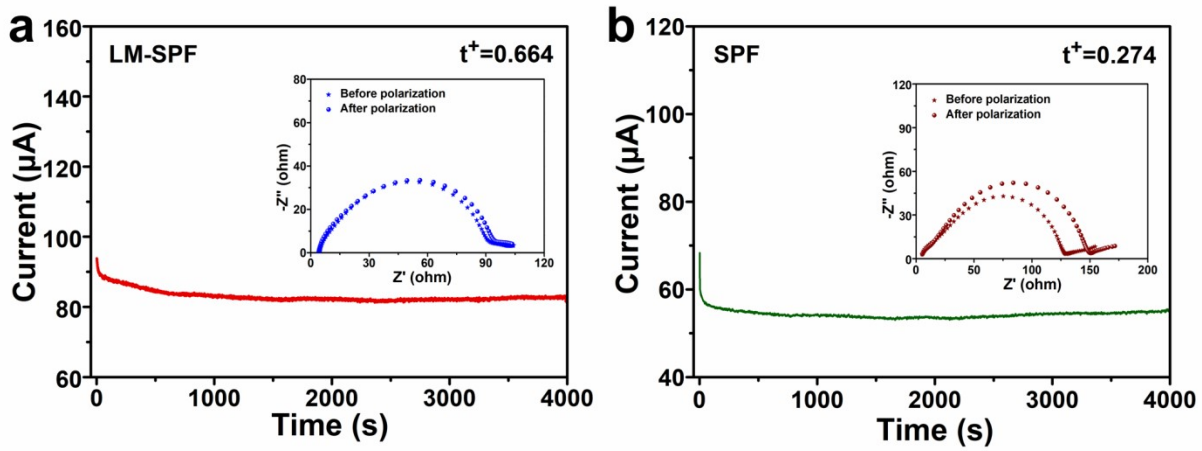

Figure S4. Current-time curves for the SPF cells, (a) LM-SPF@Li||LM-SPF@Li, and (b) SPF@Li||SPF@Li; the inset shows the EIS changes before and after polarization.

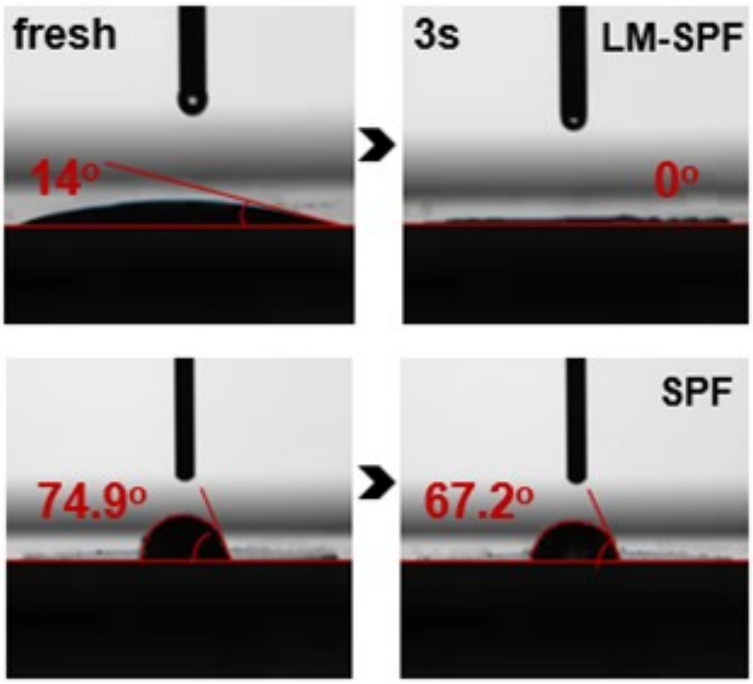

Figure S5. The corresponding wetting angle test for LM-SPF and SPF.

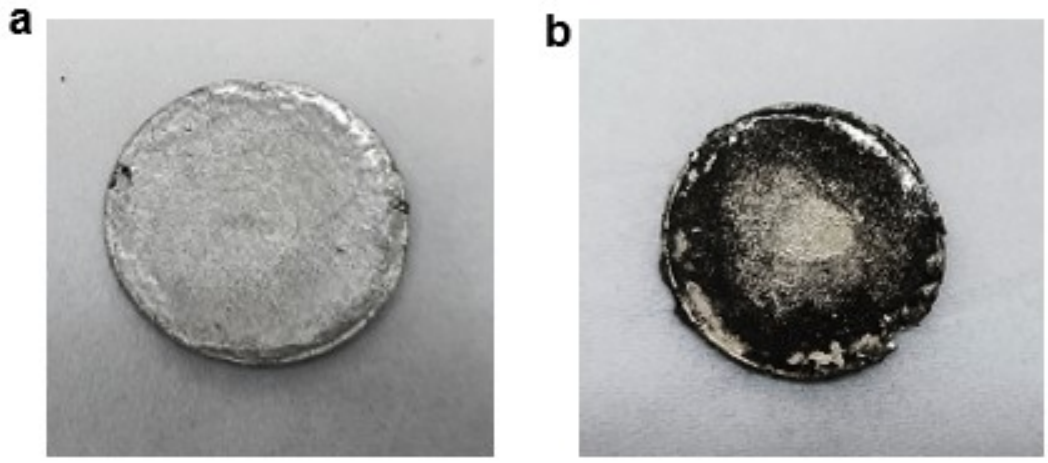

Figure S6. Optical photograph of (a) LM-SPF@Li and (b) bare Li after 100 cycles, at 2 mA cm^{-2} for 0.25 mAh cm^{-2}.

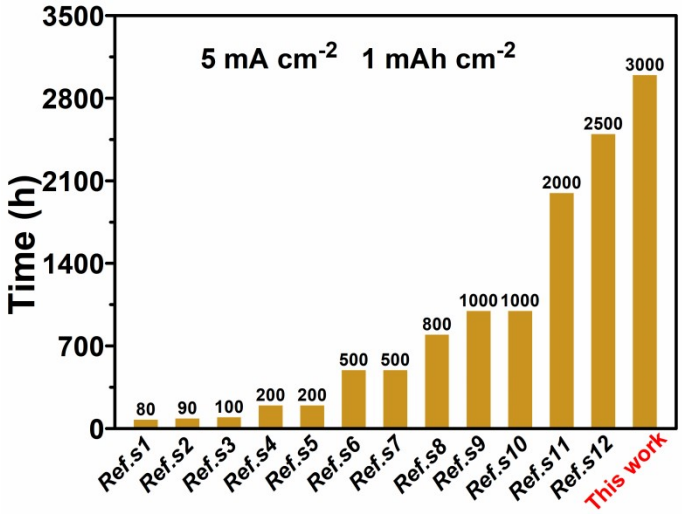

Figure S7. Comparison of the cyclic stability of LM-SPF@Li||LM-SPF@Li with that previously reported modified protective layer in Li||Li cells at the same current density and capacity.

Table S1. Comparison of the cycle stability of our LM-SPF film with that of the previously reported works.

Modified	Current density (mA cm^{-2})	Areal capacity (mAh cm^{-2})	Cycle time (h)	Ref.
TiO_2/ROLi@Li	5	1	80	1
Hybrid poly urea (HPU) film	5	1	90	2
PVDF-HFP/LiF film	5	1	100	3
PCF@Sn@Li	5	1	200	4
Nano-$AlPO_4$/PVDF-HFP film (PAF)	5	1	200	5
PTMEG/Li-Sn alloy	5	1	500	6
PMMA/PVDF	5	1	500	7
SSM@C@Li	5	1	800	8
$CaCO_3$/CNF_S@Li	5	1	1000	9
GFN_S-PVDF@PP	5	1	1000	10
Li-PEO-Upy coating	5	1	2000	11
SiO_2@PDA hybrid film	5	1	2700	12
SPF-1@Li	5	1	3000	**This work**

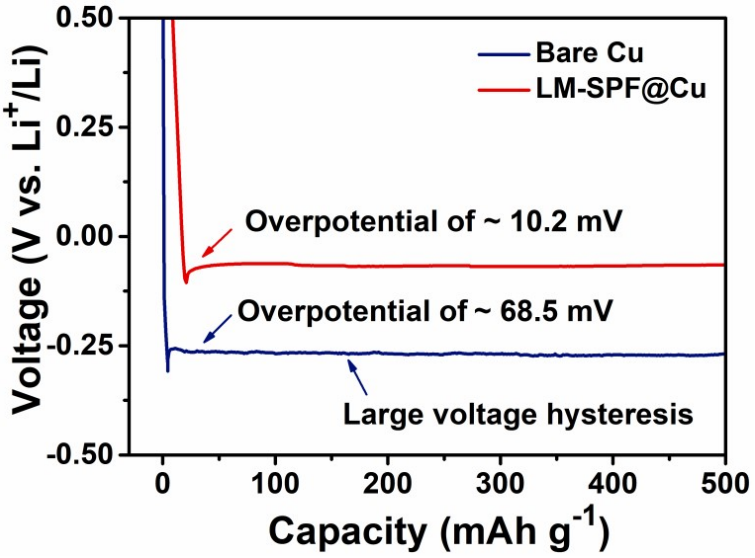

Figure S8. The voltage capacity cure corresponds to nucleation of the LM-SPF@Cu and bare Cu electrodes.

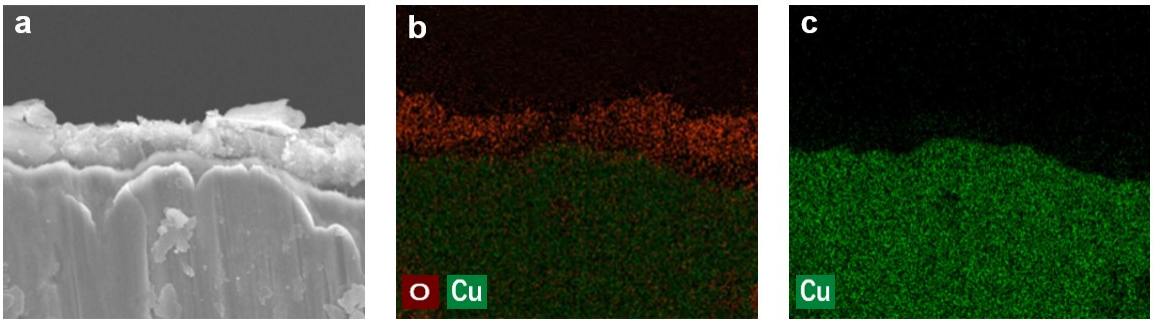

Figure S9. The morphology of the SPF-1-protected Cu cross section, after the deposition of Li with a capacity of 2 mAh cm^{-2}. (a) SEM image of the cross section of the Cu after the LM-SPF. The mapping measurements (b) and (c) revealed that lithium was deposited on a Cu foil.

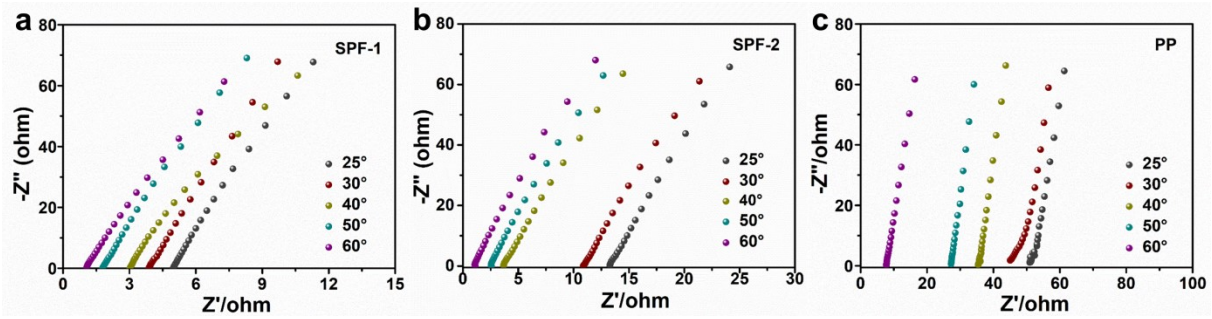

Figure S10. Nyquist plots at different temperatures of (a) SS||LM-SPF||SS, (b) SS||SPF||SS and (c) SS||PP||SS cells.

References

[1] You, J.; Deng, H.; Zheng, X.; Yan, H.; Deng, L.; Zhou, Y.; Li, J.; Chen, M.; Wu, Q.; Zhang, P.; Sun, H.; Xu, J., Stabilized and Almost Dendrite-Free Li Metal Anodes by In Situ Construction of a Composite Protective Layer for Li Metal Batteries. *ACS Appl. Mater. Interfaces* **2022,** *14* (4), 5298–5307.

[2] Sun, Y.; Amirmaleki, M.; Zhao, Y.; Zhao, C.; Liang, J.; Wang, C.; Adair, K. R.; Li, J.; Cui, T.; Wang, G.; Li, R.; Filleter, T.; Cai, M.; Sham, T. K.; Sun, X., Tailoring the Mechanical and Electrochemical Properties of an Artificial Interphase for High-Performance Metallic Lithium Anode. *Adv. Energy Mater.* **2020,** *10* (28), 2001139.

[3] Xu, R.; Zhang, X.-Q.; Cheng, X.-B.; Peng, H.-J.; Zhao, C.-Z.; Yan, C.; Huang, J.-Q., Artificial Soft-Rigid Protective Layer for Dendrite-Free Lithium Metal Anode. *Adv. Funct. Mater.* **2018,** *28* (8), 1705838.

[4] Chen, S.; Liu, T.; Ge, J.; Hong, J.; Wang, Y., Uniform Distribution of Li Deposition and High Utilization of Transferred Metallic Li Achieved by an Unusual Free-Standing Skeleton for High-Performance Li Metal Batteries. *ACS Appl. Energy Mater.* **2021,** *5* (1), 539–548.

[5] Guo, S.; Wang, L.; Jin, Y.; Piao, N.; Chen, Z.; Tian, G.; Li, J.; Zhao, C.; He, X., A polymeric Composite Protective Layer for Stable Li Metal Anodes. *Nano Converg* **2020,** *7* (1), 21.

[6] Jiang, Z.; Jin, L.; Han, Z.; Hu, W.; Zeng, Z.; Sun, Y.; Xie, J., Facile Generation of Polymer-Alloy Hybrid Layers for Dendrite-Free Lithium-Metal Anodes with Improved Moisture Stability. *Angew. Chem. Int. Ed.* **2019,** *58* (33), 11374–11378.

[7] Zhou, Z.; Feng, Y.; Wang, J.; Liang, B.; Li, Y.; Song, Z.; Itkis, D. M.; Song, J., A Robust, Highly Stretchable Ion-Conducive Skin for Stable Lithium Metal Batteries. *Chem. Eng. J.* **2020,** *396,* 125254.

[8] Zhang, Z.; Zhou, X.; Liu, Z., Conformal Coating of a Carbon Film on 3D Hosts toward Stable Lithium Anodes. *ACS Appl. Energy Mater.* **2021,** *4* (7), 7288–7297.

[9] Kim, Y.; Choi, J.; Youk, J. H.; Lee, B. S.; Yu, W. R., A Scalable, Ecofriendly, and Cost-Effective Lithium Metal Protection Layer from a Post-It Note. *RSC Adv.* **2021,** *12* (1), 346–354.

[10] Xiao, J.; Zhai, P.; Wei, Y.; Zhang, X.; Yang, W.; Cui, S.; Jin, C.; Liu, W.; Wang, X.; Jiang, H.; Luo, Z.; Zhang, X.; Gong, Y., In-Situ Formed Protecting Layer from Organic/Inorganic Concrete for Dendrite-Free Lithium Metal Anodes. *Nano Lett.* **2020,** *20* (5), 3911–3917.

[11] Wang, G.; Chen, C.; Chen, Y.; Kang, X.; Yang, C.; Wang, F.; Liu, Y.; Xiong, X., Self-Stabilized and Strongly Adhesive Supramolecular Polymer Protective Layer Enables Ultrahigh-Rate and Large-Capacity Lithium-Metal Anode. *Angew. Chem. Int. Ed.* **2020,** *59* (5), 2055–2060.

[12] Sun, X.; Yang, S.; Zhang, T.; Shi, Y.; Dong, L.; Ai, G.; Li, D.; Mao, W., Regulating Li-ion flux with a high-dielectric hybrid artificial SEI for stable Li metal anodes. *Nanoscale* **2022,** *14* (13), 5033–5043.